Electronic Supplementary Material (ESI) for Journal of Materials Chemistry C.

Armadillo-inspired Micro-foldable Metal Electrode with Negligible Resistance Change under Large Stretchability

Ziting Tan,[a] Hongwei Li,[a] Zhikai Niu,[b] Xiaosong Chen,[b] Hui Yang,[b] Weibang Lv,[a] Deyang Ji,*[b] Jie Li,*[b] Liqiang Li,*[abc] Wenping Hu[ab]

[a] *School of Nano-Tech and Nano-Bionics, University of Science and Technology of China, Hefei 230026, China.*

[b] *Tianjin Key Laboratory of Molecular Optoelectronic Sciences, Department of Chemistry, Institute of Molecular Aggregation Science, Tianjin University, Tianjin, 300072, China*

[c] *Joint School of National University of Singapore and Tianjin University, International Campus of Tianjin University, Binhai New City, Fuzhou 350207, China*

*Corresponding author. Email: lilq@tju.edu.cn; jideyang@tju.edu.cn; lijie2018@tju.edu.cn

Supporting Figures

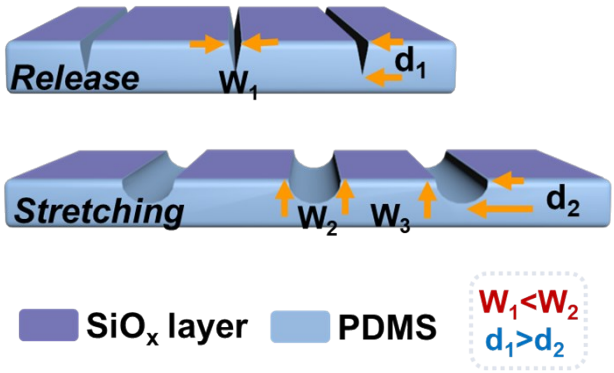

Fig. S1 Model of micro-foldable structure at folded and stretching state, respectively. It is obviously that the thickness of PDMS becomes thinner with stretching ($d_1>d_2$), and the width of the crack is wider ($W_1<W_2$).

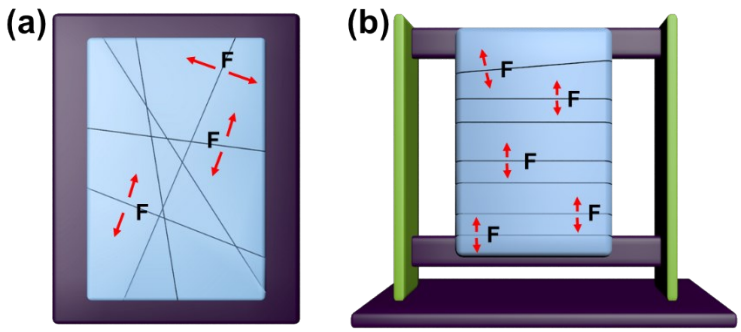

Fig. S2 PDMS is fully attached to silicon wafer (a) or suspended (b) for plasma treatment, the cracks on the surface are chaotic or uniform, respectively.

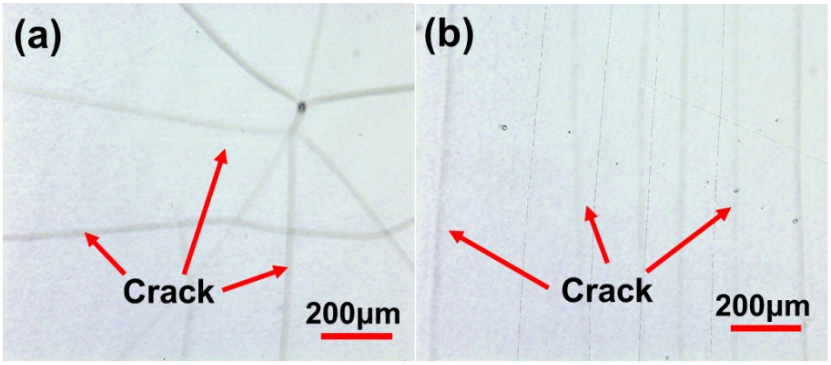

Fig. S3 3D laser scanning microscope image of (a) messy "crack" and (b) parallel structure on PDMS, which was obtained by suspending and placing on silicon wafer during oxygen plasma treatment, respectively.

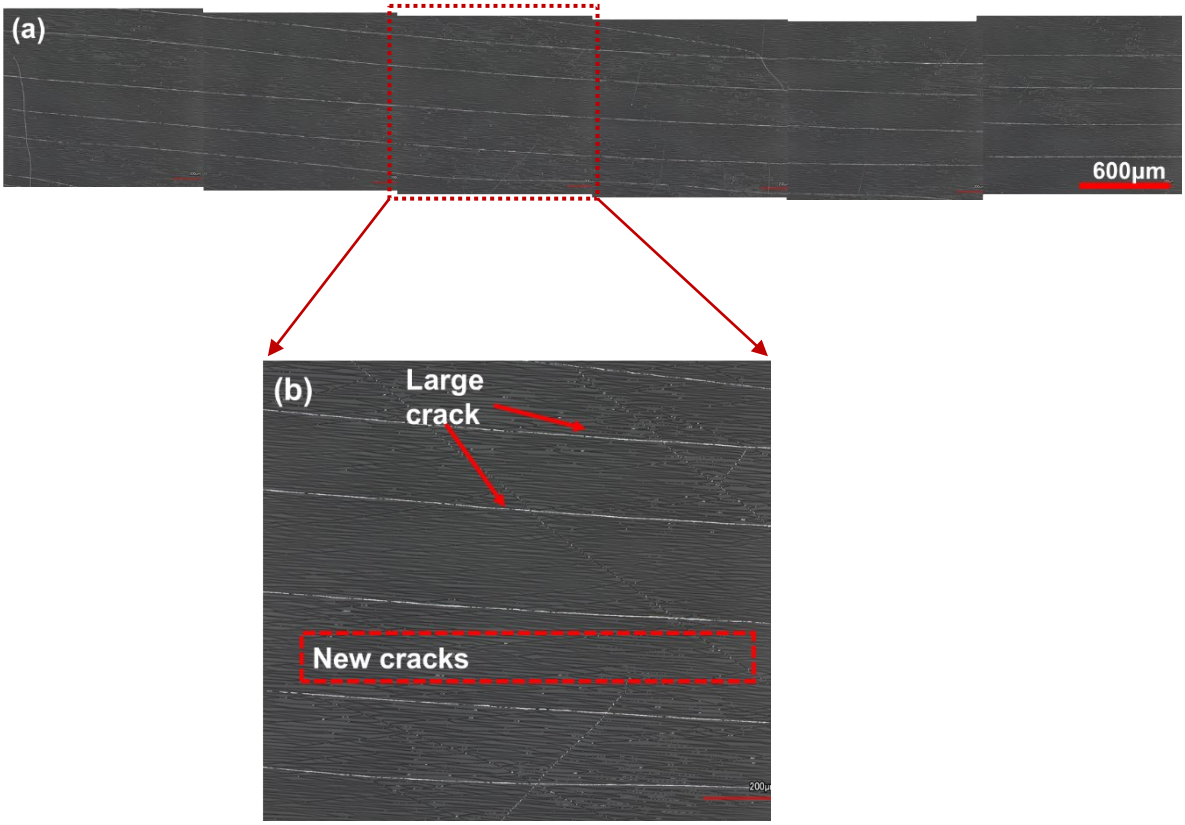

Fig. S4 3D laser scanning microscope image of parallel crack through the surface of PDMS membrane. (a) This image is combined with 6 photographs which are obtained by taking photos with microscope along the cracks. (b) enlarged part in the red framework of (a).

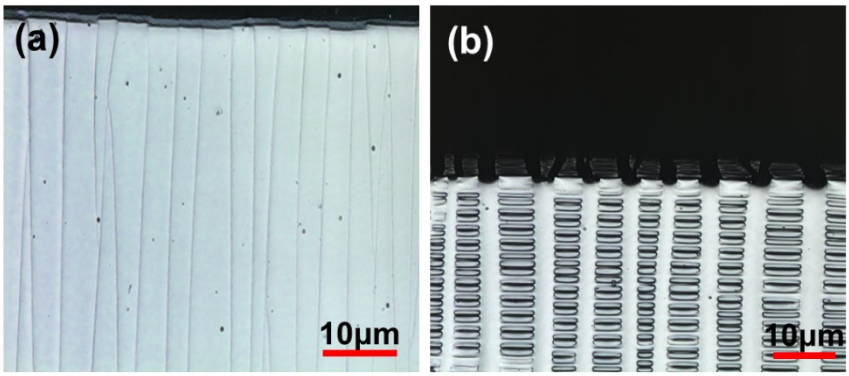

Fig. S5 (a) and (b) 3D laser scanning microscope image of "crack" structure at the edge of PDMS. (ε = 0% and 70%, respectively).

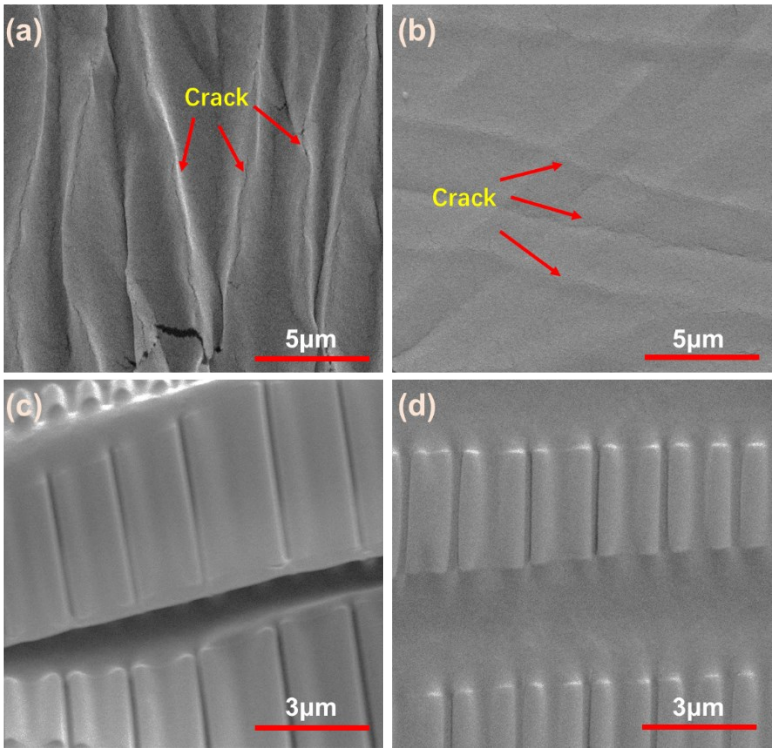

Fig. S6 Scanning electron microscopy (SEM) image of the stretchable gold electrode prepared with (a,b) non-cracked PDMS and (c,d) micro-foldable structure, respectively, both of which modify with MPTMS before deposit gold. The stretchable gold electrode under (a,c) relaxing and (b,d) stretching, respectively.

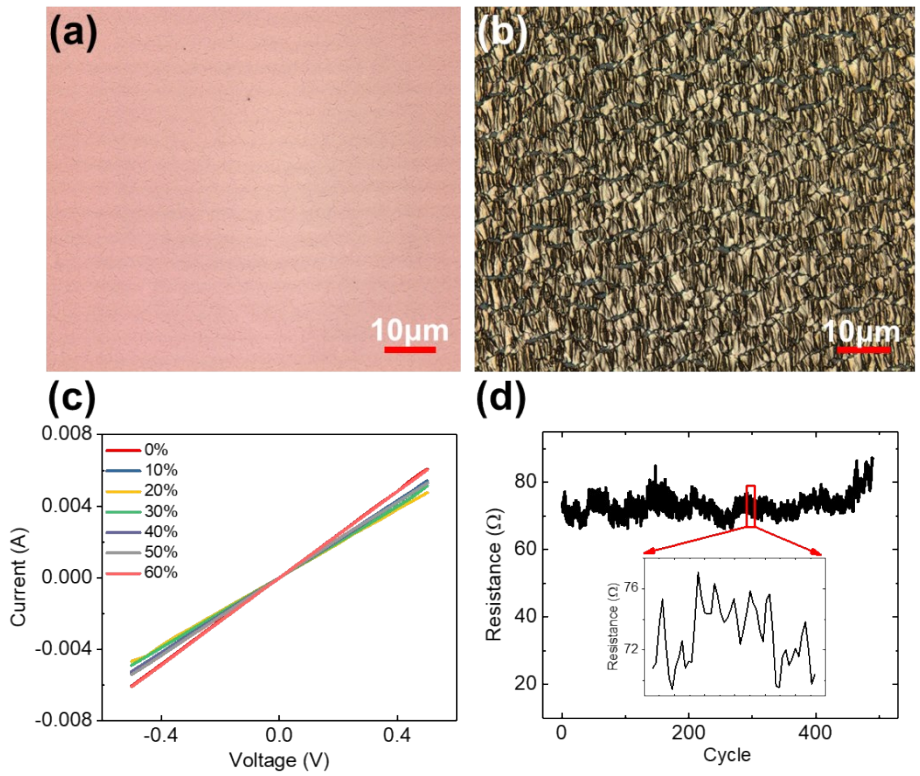

Fig. S7 The performance of electrode fabricated on non-cracked PDMS and without modifying with MPTMS. (a) and (b) Image of the gold electrode fabricated on non-cracked PDMS at stretching and releasing, respectively (c) Current-voltage curves of the gold electrode fabricated on non-cracked PDMS (d) 500 repeated stretching cycles performance under 0% to 30% tensile strain.

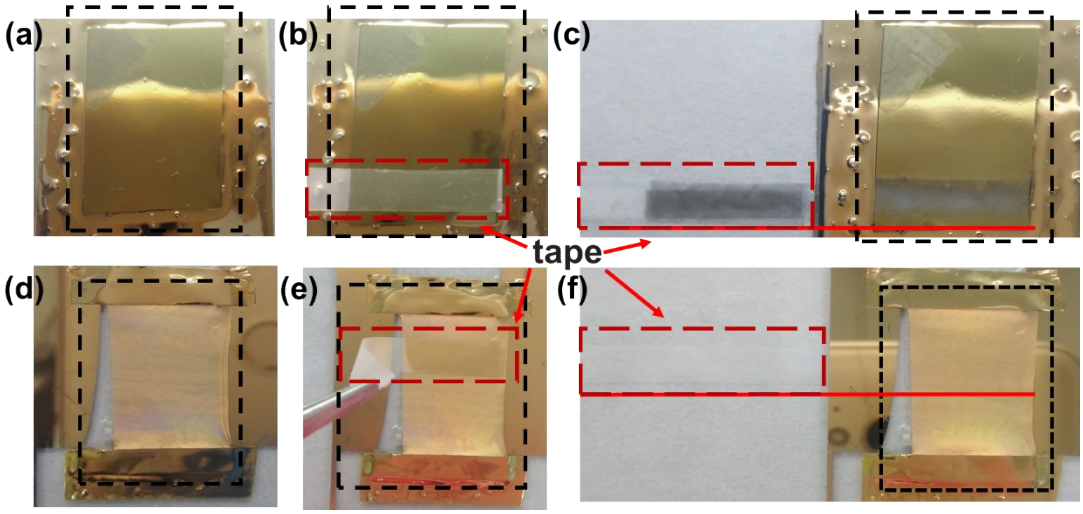

Fig. S8 Photographs of adhesion test with 3M Scotch tape. (a-c) Gold electrode fabricated on non-cracked PDMS, (d-f) Gold electrode fabricated on cracked PDMS. (a) and (d) Image of original gold electrode. (b) and (e) Image when Scotch tape tightly pasting on gold film. (c) Image after peeling off the tape from non-cracked PDMS sample. Scotch tape peels off gold film from PDMS, indicating adhesion of gold film to tape is stronger than adhesion to PDMS. (f) Image after peeling off the tape from cracked PDMS sample. Gold film is still on PDMS surface, so adhesion of gold film to PDMS is stronger than adhesion to Scotch tape.

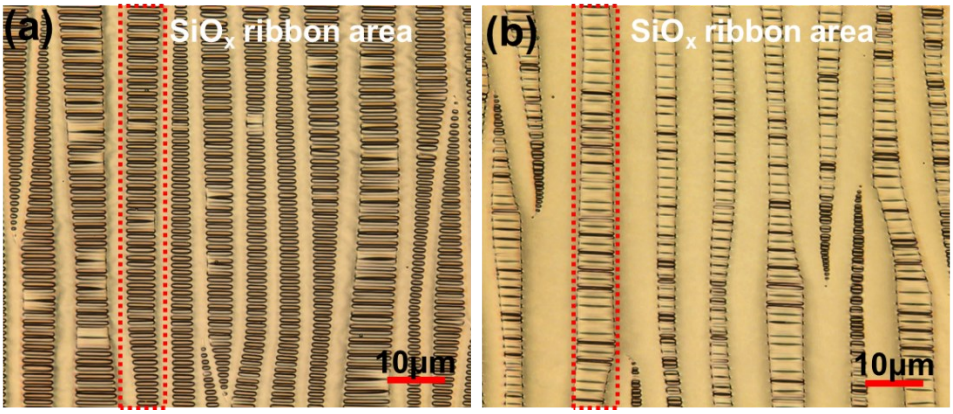

Fig. S9 SiO_x ribbon almost remain unchanged during the stretching. 3D laser scanning microscope image of stretchable gold electrode under 70% (a) and 190% (b) tensile strain, respectively.

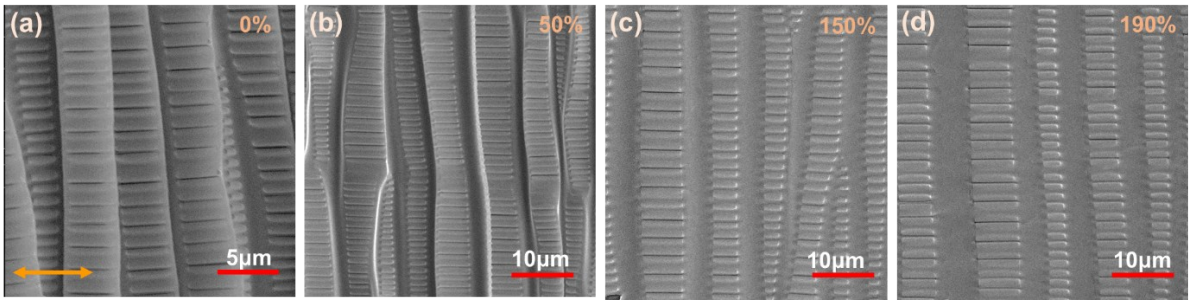

Fig. S10 Scanning electron microscopy (SEM) image of the stretchable gold electrode under (a) 0%, (b) 50%, (c) 150%, (d)190%, respectively. *Arrow pointing is uniaxial stretching direction.

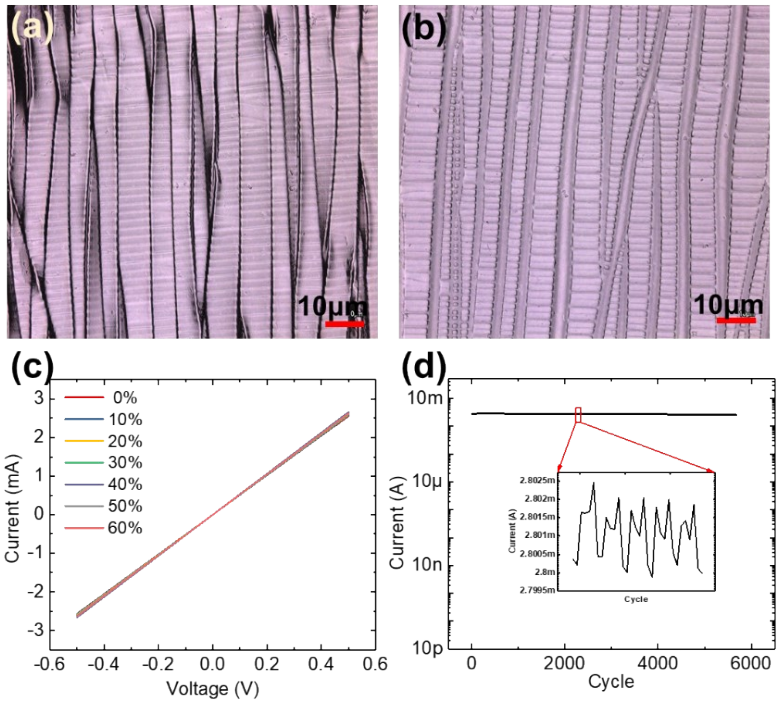

Fig. S11 (a,b) 3D laser scanning microscope image of the stretchable PEDOT:PPS electrode under relaxing and stretching, respectively. (c) The Current-voltage curves at different stretching ratios from 0% to 60%. (d) 5000 repeated stretching cycle performance under 0% to 30% tensile strain.

TableS1 Summary of some reported stretchable Au electrodes' characteristics

Material	Maximum strain	Initial resistance (R_0)	Initial conductivity σ[a] (S/cm)	Resistance under tensile strain (R_x)	Resistance change rate[b]	Formable	Durability (Cyclic test)	Ref.
Au /PDMS	40%	5.5 Ω	-	12.5 Ω (ε=10%.)	120%	Nanopile Interlocking	1000	[1]
Au /PDMS	100%	95 Ω	-	530Ω (ε=100%.)	450%	Fibers	1000	[2]
Au@PVP/ PDMS	140%	100 Ω	-	242 Ω (ε=140%)	140%	Buckled nanofiber networks	3000	[3]
Au nanomesh/ PDMS	160%	25 Ω/□	10500	67Ω/□ (ε=160%)	160%	Au nanomesh	1000	[4]
Au nanomesh/ PDMS	160%	20−30 Ω/□	8771-13000	46-69 Ω/□ (ε=160%)	130%-	Au nanomesh	25000	[5]
Au nanomesh/ PDMS	300	28 Ω/□	9398	72.8 Ω/□ (ε=300%)	160%	Au nanomesh	50000	[6]
Au nanobelt/ Tripod PDMS	130%	25 Ω	-	Nearly no change	-	Suspended gold nanobelts	10000	[7]
Au Nanosheets/ Ecoflex	200%	6.0×10^{-6}Ω m	1600	9.6×10^{-6}Ω m (ε=100%)	60%	Au Nanosheets	3000	[8]
Au Nanoframework/ PDMS	420%	100 Ω/□	2631	300 Ω/□ (ε=100%)	200%	Fractal Gold Nanoframework	100000	[9]
Au/PDMS	200%	16.9 Ω/□	15000	118.3 Ω/□ (ε=120%)	600%	High Aspect Ratio Serpentine Structure	100	[10]
Micro-folded Au film	**190%**	**4.39 Ω**	**42000**	**4.96Ω (ε=190%)**	**13%**	**Foldable thin film**	**10000**	**This work**

[a]$\sigma = {}^{1}/_{(38\ nm * R_{\square})}$ (Defining the thickness of the gold film for all example to be 38nm; [b]Resistance change rate = (R_x-R_0)/R

Experimental section

Sample. Polydimethylsiloxane (PDMS), (Sylgard 184 from Dow Corning); Perfluorooctyltrichlorosilane (FOTCS) (from J&K Scientific); (3-mercaptopropyl) trimethoxysilane (MPTMS), from Sigma Aldrich.

Fabrication of Stretchable Electrodes and Capacitive Sensors. The curing agent and the base material at a ratio of 1:10 by mass were mixed thoroughly to produce the silicone elastomer PDMS samples. The mixture was cured in a 1.2 inch silicon wafer, which was pre-silanized in FOTCS, and then annealed at 80 ℃ in an oven for 1 hour to form the PDMS. Then, the PDMS samples were treated with O_2 Plasma (27 mbar, 150 W, for 10 minutes) in the state of being fixedly suspended at both ends to generate the silica-like surface layer and parallel microscale large cracks. After that, the PDMS membrane were stretched to further form new cracks and modification with MPTMS for 1 hour under pre-stretching state.[11,12] Finally, 40 nm-thickness gold was deposited on it in thermal evaporator under certain pre-stretched state to form the stand-by stretchable electrode. Capacitive sensors were prepared by coating the gold film onto double side. The both ends of the pre-stretched PDMS film are fixed on the square frame, and deposit the gold film twice on both sides of the PDMS. In this work, we optimized the time of oxygen plasma treatment and the thickness of PDMS. As shown in Figure S10, the formation of the cracks was affected by the treating time of oxygen plasma. When the PDMS substrate was treated with oxygen plasma for 5, 10, 15 minutes, respectively, different cracks on the surface of PDMS would be form (Fig. S12a-c). As a result, the sample treated for 10 minutes exhibited the most stable electrical performance (Fig. 3c and Fig. S12e, f). This may be related to the fact that shallow cracks occur in short treating time, whereas long-term treatment results in chaotic and deep cracks on PDMS. If the crack is shallow, gold crowds in cracks, which squeezes the gold film to break when electrode relaxes. On the other hand, PDMS surface with messy and deep cracks may induce the gold film to break in various direction after repeated stretching, which may greatly sacrifice electrical stability. Additionally, we fabricated the stretchable gold electrode on 150 μm and

200 μm thick cracked-PDMS (Fig. S13), and founded that the thickness of PDMS did not affect the electrical performance of the stretchable gold electrode. It is reasonable because the cracked PDMS surface mainly determines the stretchable property and the rest PDMS layer mainly work as elastic supporting substrate.

Characterization of Stretchable Electrodes and Capacitive Sensor. Electrical performance of stretchable electrodes was measured in ambient conditions using a Keithley 4200-SCS. The two ends of the electrode were clamped by two clips horizontally, and stretched or released under the movement of high-precision stepper motor (Beijing Optical Century Instrument Co., Ltd., SC100).[13] A light-emitting diode (LED) was connected with stretchable electrode for direct observation. The Au-PDMS-Au capacitive sensor was clamped as stretchable electrode and fixed on the middle finger joint to carry out the electrical characterization in ambient conditions by Keysight E4980AL (at 100 kHz). The stretchable electrodes were equipped on the forearm for EMG detecting and signals were recorded by a commercial detector (TrueSense V1.1).

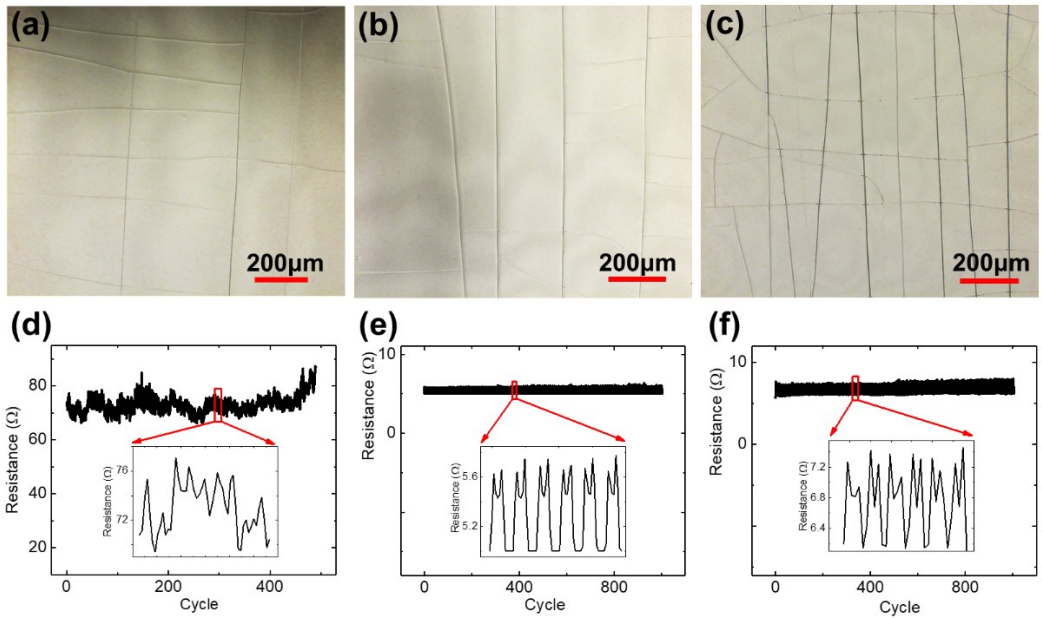

Fig. S12 Influence of treating time of oxygen plasma. (a-c) 3D laser scanning microscope image of "crack" structure on PDMS, which was treated by oxygen plasma for 5 min, 10 min and 15 min, respectively; (d-f) Cycle performance of the samples, which were fabricated on the PDMS treated with oxygen plasma for 0 min, 5 min and 15 min, respectively.

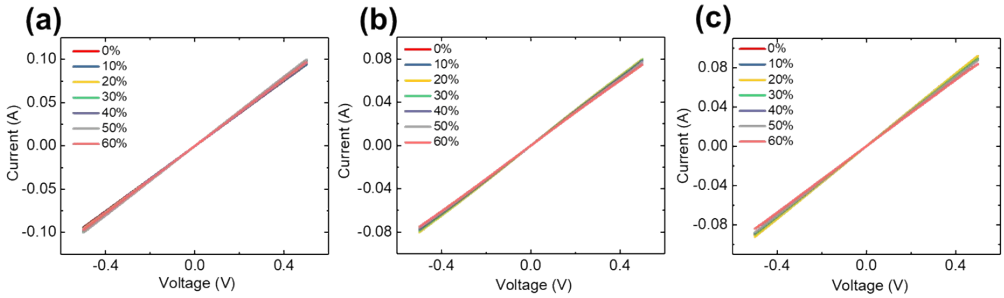

Fig. S13 The effect of thickness of PDMS. (a-c) Current-voltage curves of stretchable gold electrode on PDMS with different thickness of 100 μm, 150 μm, and 200 μm, respectively.

Reference

1 Z. Liu, X. Wang, D. Qi, C. Xu, J. Yu, Y. Liu, Y. Jiang, B. Liedberg, X. Chen, *Adv. Mater.,* 2017, **29**, 1603382.
2 B. Zhang, J. Lei, D. Qi, Z. Liu, Y. Wang, G. Xiao, J. Wu, W. Zhang, F. Huo, X. Chen, *Adv. Funct. Mater.*, 2018, **28**, 1801683.
3 Y. Jin, S. Hwang, H. Ha, H. Park, S.-W. Kang, S. Hyun, S. Jeon, S.-H. Jeong, *Adv. Electron. Mater.,* 2016, **2**, 1500302.
4 C. Guo, T. Sun, Q. Liu, Z. Suo, Z. Ren, *Nat. Commun.,* 2014, **5**, 3121.
5 C. Guo, Y. Chen, L. Tang, F. Wang, Z. Ren, *Nano Lett.*, 2016, **16**, 594.
6 C. Guo, Q. Liu, G. Wang, Y. Wang, Z. Shi, Z. Suo, C.-W. Chu, Z. Ren, *Proc. Natl. Acad. Sci. U. S. A.,* 2015, **40**, 12332.
7 D. Qi, Z. Liu, M. Yu, Y Liu, Y. Tang, J. Lv, Y. Li, J. Wei, B. Liedberg, Z. Yu, X. Chen, *Adv. Mater.,* 2015, **27**, 3145.
8 G. D. Moon, G.-H. Lim, J. H. Song, M. Shin, T. Yu, B. Lim, U. Jeong, *Adv. Mater.,* 2013, **25**, 2707.
9 M. D. Ho, Y. Liu, D. Dong, Y. Zhao, W. Cheng, *Nano Lett.*, 2018, **18**, 3593.
10 S. Jang, C. Kim, J. J. Park, M. L. Jin, S. J. Kim, O.O. Park, T.-S. Kim, H.-T. Jung, *Small*, 2018, **14**, 1702818.
11 Y. Ogawa, T. Niu, S.L. Wong, M. Tsuji, A.T.S. Wee, W. Chen, H. Ago, *J. Phys. Chem. C,* 2013, **117**, 21849.
12 Z. Zhang, X. Ren, B. Peng, Z Wang, X. Wang, K. Pei, B. Shan, Q. Miao, P.K.L. Chan, *Adv. Funct. Mater.,* 2015, **25**, 6112.
13 H. Li, K. Wu, Z. Xu, Z. Wang, Y. Meng, L. Li, Ultrahigh-sensitivity piezoresistive Pressure sensors for detection of tiny pressure. *ACS Appl. Mater. Interfaces*, 2018, **10**, 20826.